tvst

DOI: 10.1167/tvst.5.1.8

Article

Two Bioactive Molecular Weight Fractions of a Conditioned Medium Enhance RPE Cell Survival on Age-Related Macular Degeneration and Aged Bruch's Membrane

Ilene K. Sugino[1], Qian Sun[1], Carola Springer[1], Noounanong Cheewatrakoolpong[1], Tong Liu[2], Hong Li[2], and Marco A. Zarbin[1]

[1] Institute of Ophthalmology and Visual Science, Rutgers, New Jersey Medical School, Newark, NJ, USA
[2] Department of Biochemistry and Molecular Biology, Center for Advanced Proteomics Research, Neuroproteomics Core Facility, Rutgers, New Jersey Medical School, Newark, NJ, USA

Correspondence: Marco A. Zarbin, Institute of Ophthalmology and Visual Science, 90 Bergen Street, Newark, NJ 07101-1709, USA; zarbin@earthlink.net

Received: 4 September 2015
Accepted: 1 January 2016
Published: 22 February 2016

Keywords: age-related macular degeneration; retinal pigment epithelium; cell transplantation; Bruch's membrane; cell survival

Citation: Sugino IK, Sun Q, Springer C, et al. Two bioactive molecular weight fractions of a conditioned medium enhance RPE cell survival on age-related macular degeneration and aged Bruch's membrane. 2016;5(1):8, doi:10.1167/tvst.5.1.8

Purpose: To characterize molecular weight fractions of bovine corneal endothelial cell conditioned medium (CM) supporting retinal pigment epithelium (RPE) cell survival on aged and age-related macular degeneration (AMD) Bruch's membrane.

Methods: CM was subject to size separation using centrifugal filters. Retentate and filtrate fractions were tested for bioactivity by analyzing RPE survival on submacular Bruch's membrane of aged and AMD donor eyes and behavior on collagen I-coated tissue culture wells. Protein and peptide composition of active fractions was determined by mass spectrometry.

Results: Two bioactive fractions, 3-kDa filtrate and a 10-50–kDa fraction, were necessary for RPE survival on aged and AMD Bruch's membrane. The 3-kDa filtrate, but not the 10-50–kDa fraction, supported RPE growth on collagen 1-coated tissue culture plates. Mass spectrometry of the 10-50–kDa fraction identified 175 extracellular proteins, including growth factors and extracellular matrix molecules. Transforming growth factor (TGF)β-2 was identified as unique to active CM. Peptides representing 29 unique proteins were identified in the 3-KDa filtrate.

Conclusions: These results indicate there is a minimum of two bioactive molecules in CM, one found in the 3-kDa filtrate and one in the 10-50–kDa fraction, and that bioactive molecules in both fractions must be present to ensure RPE survival on Bruch's membrane. Mass spectrometry analysis suggested proteins to test in future studies to identify proteins that may contribute to CM bioactivity.

Translational Relevance: Results of this study are the first steps in development of an adjunct to cell-based therapy to ensure cell transplant survival and functionality in AMD patients.

Introduction

In the advanced form of dry age-related macular degeneration (AMD), termed geographic atrophy (GA), retinal pigment epithelium (RPE) cells are dysfunctional and die with associated loss of photoreceptors. The area of RPE atrophy generally starts in the parafoveal region and may eventually affect the fovea as the defect progresses. RPE replacement may be a treatment to prevent further vision loss and potentially improve vision in areas at the edge of GA, where the RPE are dying/dysfunctional and the photoreceptors are not fully degenerate. Clinical trials are underway using RPE derived from embryonic stem cells (ESC-RPE) and from induced pluripotent stem cells (iPSC-RPE) to treat patients with AMD.[1]

Recently published results from clinical trials using ESC-RPE demonstrated the safety of RPE cell suspension transplants.[2,3] The ESC-RPE were transplanted in the region straddling the area of GA. Postoperative images showed presumptive ESC-RPE primarily along and near the edge of the GA-associated RPE defect and not in the area of GA. Results from these clinical trials indicate that most of the transplanted ESC-RPE were unable to survive on and resurface areas of GA, where abnormal Bruch's

membrane, the surface on which RPE normally reside, is exposed. An organ culture assay using human donor eyes demonstrates similar findings: most transplanted RPE cells do not survive on human Bruch's membrane in areas affected by AMD, including areas of GA.[4] Thus, interventions that improve long-term RPE cell survival on Bruch's membrane in areas of GA may lead to better visual results in patients undergoing RPE transplantation for advanced dry AMD.

We have found that a conditioned medium (CM) derived from bovine corneal endothelial cells (BCEC) dramatically improves ESC-RPE and fetal RPE cell survival on AMD Bruch's membrane, including in areas of GA.[4] When CM is used as a culture medium, survival of morphologically differentiated RPE is evident 21 days after transplantation on aged, as well as AMD Bruch's membrane of human donor eyes (including in areas of GA as well as in areas from which choroidal new vessels have been surgically excised), while survival is poor in cultures where standard RPE culture medium is used.[4–6]

Here, we report studies using cell and organ culture assays to identify the bioactive fractions of CM and mass spectrometry studies to identify the composition of the bioactive fractions. We also compared the protein composition of active versus inactive CM to assess qualitative differences in the two mixtures. The results of this study are the first steps toward developing a mixture of molecules that may be used as an adjunct to RPE replacement therapy to treat patients with AMD by improving grafted cell survival, thereby making cell transplants more effective.

Material and Methods

This research was ruled exempt (nonhuman subjects research) by the institutional review board of Rutgers, the State University of New Jersey.

Conditioned Medium Manufacture and Filtration Fractionation

BCEC were isolated from corneas of young slaughterhouse cows (approximate age, 6 months) and cultured as previously described.[4] CM was harvested from passage 2 cultures after 72-hour exposure to Madin-Darby Bovine Kidney Maintenance Medium (MDBK-MM [referred to hereafter as "CM vehicle"]; Excell custom medium, Sigma-Aldrich, St. Louis, MO). Following harvest, CM was briefly centrifuged to remove cellular debris, aliquoted, and stored at −80°C. Bioactivity of each CM batch was confirmed by the Bruch's membrane bioassay (see below). A total of 20 different CM preparations were used for the Bruch's membrane bioassay studies in which bioactive fractions were identified.

CM was separated into fractions using centrifugal filters of sizes 3 to 300 kDa (Amicon Ultra 4; EMD Millipore, Billerica, MA). Prior to CM size separation, filters were blocked with 5% bovine serum albumin solution (BSA) in phosphate-buffered saline (PBS, Sigma-Aldrich) containing 2.5 μg/mL amphotericin B and 50 μg/mL gentamicin (both from Life Technologies, Carlsbad, CA) for 1 hour at room temperature followed by washing with PBS containing amphotericin B and gentamicin. Each filter generates two fractions, a retentate, comprising molecules above the exclusion molecular weight of the filter, and a filtrate, comprising molecules below the exclusion molecular weight of the filter. Because the retentate is concentrated following filtration, it was reconstituted to the starting volume by the addition of CM vehicle or a low molecular weight CM fraction.

Fetal RPE Culture

Human fetal eyes (17- to 22-weeks gestation) were obtained from Advanced Biosciences Resources, Inc. (ABR; Alameda, California). RPE cells were isolated using collagenase IV and cultured on BCEC extracellular matrix (ECM) according to previously published methods.[7–9] RPE cells were cultured in medium containing Dulbecco's modified Eagle's medium (DMEM; Cellgro, Manassas, VA) supplemented with 2 mM glutamine, 15% fetal bovine serum, 2.5 μg/mL amphotericin B, 50 μg/mL gentamicin, and 1 ng/mL bFGF (all from Life Technologies). Cultured RPE cells were harvested from early passage cultures (P1–4) after short times in culture (3–7 days) for seeding onto Bruch's membrane and for the cell culture experiments described below.

Bruch's Membrane Bioassay

A total of 92 submacular explants were prepared from the eyes of 64 donors (mean age, 78.4 ± 8.3 years for CM fraction testing (see Supplement Table S1 for donor information). Five additional donor eyes (mean donor age 80.4 ± 2.7 years: 3 donors with no pathology, 1 donor with extramacular hard drusen, 1 donor with GA) were prepared for studies examining

RPE cell behavior on explants that were subject to a freeze/thaw cycle. Donor eyes were obtained from the Lions Eye Institute for Transplant and Research (Tampa, FL), National Disease Research Interchange (Philadelphia, PA), and Midwest Eye-Banks (Ann Arbor, MI). Acceptance criteria for donor eyes included: (1) death to enucleation time no more than 7 hours, (2) death to receipt time no more than 48 hours, (3) no ventilator support prior to death, (4) no chemotherapy within the last 6 months prior to death, (5) no radiation to the head within the last 6 months prior to death, (6) no recent head trauma, and (7) no ocular history affecting the posterior segment except for AMD. In previous studies, these acceptance criteria have been found to yield well-preserved explants.[4–6] Explants comprising choroid and sclera were debrided using a moistened surgical sponge to remove native RPE cells and subjacent basement membrane, exposing the surface of the inner collagenous layer (ICL).[7] Macula-centered 6-mm Bruch's membrane explants were placed in 96-well plates and seeded with 3164 RPE cells/mm^2. Explants were cultured for 21 days. This incubation period was chosen because the beneficial effect of culture in CM increases with time in culture. As shown previously, significantly greater RPE cell survival and resurfacing (reflected in nuclear density counts) are seen in 21- versus 7- or 14-day culture.[4]

At day 21, explants were fixed in cold phosphate-buffered 2% paraformaldehyde and 2.5% glutaraldehyde. Explants that were analyzed for light and scanning electron microscopy (SEM) were bisected for processing.

Explant Analysis

Explants for SEM analysis were dehydrated, critical point dried, and sputter-coated according to standard procedures. Explants were imaged (JEOL JSM 6510; Tokyo, Japan) routinely at low magnification (×30, ×50) for assessment of coverage and at higher magnification (×200, ×1000) to visualize the central 3 mm of the explant. Image analysis at these higher magnifications focused on surface morphology of RPE cells, assessment of RPE coverage (to be correlated with light microscopy analysis), and evaluation of the Bruch's membrane surface in areas not covered by RPE cells.

Explants for light microscopic evaluation were processed and embedded in LR White (Electron Microscopy Sciences, Hatfield, PA). Nuclear density counts, a measure of RPE survival on submacular Bruch's membrane, were performed on 2-μm thick sections stained with toluidine blue as previously described.[4] Nuclear densities were expressed as the average number of nuclei per millimeter of submacular Bruch's membrane (±standard error). Sections were also evaluated for RPE cell morphology and integrity of Bruch's membrane and choroid.

Nuclear densities and donor ages of each group were compared for statistical significance ($P < 0.05$) by Mann-Whitney Rank Sum Test for comparisons between two groups and Kruskal-Wallis ANOVA on Ranks for comparisons between multiple groups. If significance was observed following ANOVA on Ranks comparisons, All Pairwise Multiple Comparison Procedures testing (Dunn's method) determined the significance between pairs of groups. SigmaPlot 12.5 (Systat Software, Inc., San Jose, CA) was used for statistical analysis.

Cell Culture Assay

Fetal RPE cells at the same density used for seeding onto Bruch's membrane explants (3164 RPE cells/mm^2) were seeded onto human collagen I-coated tissue culture wells (BD Bioscience, Bedford, MA) and cultured in CM fractions from three different CM batches. Control dishes were cultured in CM vehicle (MDBK-MM). Wells were photographed at day 1, 3, 7, 14, and 21.

Mass Spectrometry

Bioactive fractions (3-kDa filtrate, 3 different CM preparations and 10-50–kDa fraction, 4 different CM preparations each of active and inactive CM) were analyzed by mass spectrometry. Proteins of the 10-50–kDa fraction were acetone-precipitated and desalted (ReadyPrep 2-D Cleanup Kit; Bio-Rad Laboratories, Inc., Hercules, CA). In-solution digestion with trypsin was performed on the 10-50–kDa proteins and half of the volume of the 3-kDa filtrates (the remaining half of the 3-kDa filtrates was analyzed without trypsin digestion). All samples were further desalted (Pierce C18 Spin Column; Thermo Fisher Scientific, Rockford, IL). Samples were analyzed by LC-MS/MS (liquid chromatography-tandem mass spectrometry) (LTQ Orbitrap Velos; Thermos Fisher Scientific) in a data-dependent acquisition mode. After each MS scan, the top 15 intensity ions were selected for MS/MS analysis using HCD (higher energy collusional dissociation) fragmentation. The MS/MS spectra were searched against an IPI bovine database (IPI, www.edi.ac.uk/IPI) using MASCOT (V.2.3) search engine (Matrix Science, Inc., Boston, MA). The oxidation (M) and carbamidomethyl (C) were set as variable modifications. Proteins were identified by peptide identifi-

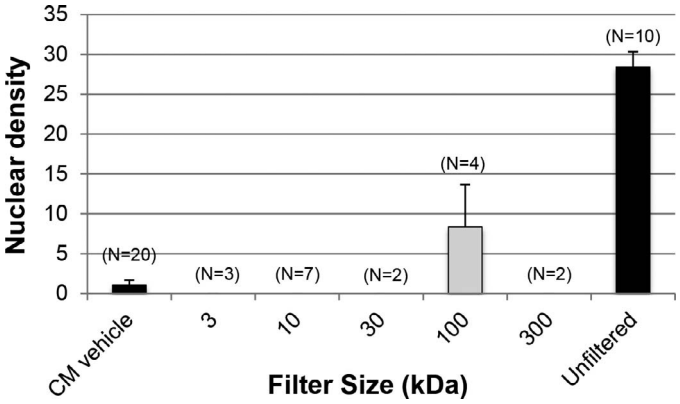

Figure 1. Nuclear density (mean number of nuclei/mm Bruch's membrane) following 21-day RPE cell culture in high molecular weight retentates (i.e., material of molecular weight ≥filter size). Nuclear densities of retentates were not significantly different from the nuclear density following culture in CM vehicle ($P = 0.206$, ANOVA on Ranks). Nuclear density after culture in CM vehicle and unfiltered CM are included for comparison.

cation with a probability greater than 95%. (The protein false discovery rate was less than 1%.) IPI identification codes were mapped to Uniprot identification codes (http://www.uniprot.org), and location and function of identified proteins were determined by pathway analysis software (IPA; Ingenuity Systems, Inc., Redwood City, CA). Location and function of unmapped proteins and peptides were determined by database identification (www.genecards.org).

Results

Fetal RPE Survival on Bruch's Membrane Following Culture in CM Fractions

Culture in Molecular Cut Filter Retentates

Nuclear densities of RPE cells seeded on submacular Bruch's membrane after 21-day culture in molecular cut filter retentates were not significantly different than the nuclear density of RPE cells cultured in CM vehicle (Fig. 1). Most explants cultured in CM retentate fractions or CM vehicle were devoid of cells on the ICL or had varying amounts of cellular debris on the ICL surface, including remnants of cells (Fig. 2A). However, while two of four explants cultured in the 100-kDa retentate had no cells, the remaining two explants were partially resurfaced by very large, flat cells with nuclear densities of 11.3 and 22.2 (shown in Fig. 2B) nuclei/mm Bruch's membrane. Of the 20 explants cultured in CM vehicle, 16 explants had no cells remaining on the ICL surface, two explants were resurfaced by rounded, single cells, the majority of which did not have intact plasma membrane, and two explants had patches of extremely flat but intact cells at one explant edge. Comparison of donor ages between groups showed no statistically significant differences ($P = 0.106$). These results show that, regardless of the size of the filtration filter, retentates

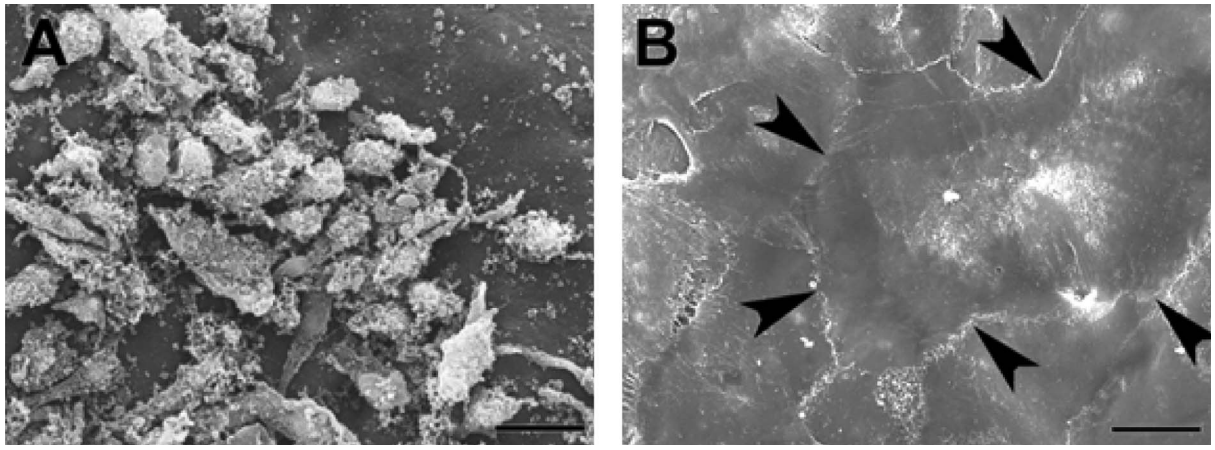

Figure 2. Morphology of RPE cells remaining after 21-day culture on aged submacular Bruch's membrane in high molecular weight CM retentates. (A) RPE cells cultured in the 3-kDa retentate on this explant were present as cell clumps on the ICL surface. The cells were not spread and plasma membranes were not intact. Nuclear density of this explant was 0 (the cells were not well attached and fell off during the processing for nuclear density counting). The donor was an 82-year-old Caucasian female with a few submacular drusen. (B) RPE cells cultured in the 100-kDa retentate on two explants were mostly intact. This explant (highest nuclear density of explants cultured in 100-kDa retentate) was almost fully resurfaced by very large, flat cells (*arrowheads* point to the border of a very large cell that exhibited small holes in its plasma membrane). Nuclear density was 22.2 ± 0.97 nuclei/mm Bruch's membrane. The donor was a 72-year-old Caucasian female with no submacular pathology. *Magnification bar*, 20 μm.

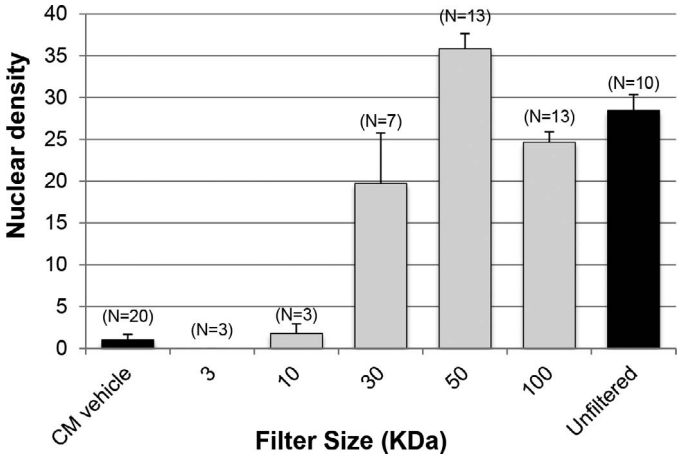

Figure 3. Nuclear densities of fetal RPE cells following 21-day culture in filtrates (i.e., material of molecular weight <filter size). Nuclear density culture in 3- and 10-kDa filtrates were not significantly different from RPE cells cultured in CM vehicle and were significantly lower than the nuclear density of cells cultured in unfiltered CM. Filtrates nuclear densities of 30, 50, and 100 kDa were significantly higher than CM vehicle nuclear densities. Nuclear densities of 30 and 100 kDa were similar to unfiltered CM nuclear density, while the 50-kDa nuclear density was significantly higher than unfiltered CM nuclear density and the nuclear densities resulting from the 30- and 100-kDa filtrates (comparisons were considered significant if $P < 0.05$; Mann-Whitney Rank Sum Test and Kruskal-Wallis ANOVA on Ranks).

support no or limited RPE cell survival on explants. Because no cell survival was seen in the retentate generated by the 3-kDa filter, these results indicate that there is a low molecular weight fraction found in the 3-kDa filtrate that is critical for CM effectiveness.

Culture in Molecular Cut Filter Filtrates

The nuclear density of cells cultured in molecular cut filter filtrates resulting from the 3- and 10-kDa filters were similar to the nuclear density of cells cultured in CM vehicle ($P = 0.447$ and 0.140, respectively). Higher molecular weight filtrates from the 30-, 50-, and 100-kDa filters showed nuclear densities significantly higher than the nuclear densities resulting from culture in CM vehicle ($P = 0.003$, $P < 0.001$, $P < 0.001$, respectively). The 30- and 100-kDa filtrate nuclear densities were similar to the nuclear densities of unfiltered CM ($P = 0.261$ and 0.251, respectively), but the nuclear density resulting from culture in the 50-kDa filtrate was significantly higher than the nuclear density after culture in unfiltered CM ($P = 0.020$), 30-kDa filtrate ($P = 0.026$), or 100-kDa filtrate ($P = <0.001$; Fig. 3). There were no significant differences between the donor ages of groups ($P = 0.0.072$). These results indicate that the 50-kDa filtrate contains molecules contributing to the biological effect of CM, and because significant bioactivity of CM is lost in the 10-kDa filtrate, a molecular fraction containing significant CM bioactivity is in the 10-50–kDa fraction.

Most explants cultured in the 3- and 10-kDa filtrates exhibited bare ICL. One explant, cultured in 10-kDa filtrate, was resurfaced by a few patches of very flat cells on the ICL (nuclear density, 3.94 ± 0.52 nuclei/mm Bruch's membrane, not shown). Explants cultured in the 30-kDa filtrate were highly variable in nuclear density, ranging from no surviving RPE to almost fully resurfaced (0–41.4 nuclei/mm Bruch's membrane). Of the four explants with RPE on the ICL surface, RPE cells were mono- or multilayered and highly variable in morphology, ranging from small, flat cells to large, flat cells (Figs. 4A, 4B).

RPE cells cultured in the 50-, 100-kDa filtrate, or unfiltered CM resurfaced Bruch's membrane with a mixture of cells of different sizes. Explants cultured in the 50-kDa filtrate tended to exhibit more mature, small cells than those cultured in the 100-kDa filtrate or in unfiltered CM (Figs. 4C, 4D, 5, and 6). Large, ballooned cells (Fig. 5B) were present in some explants, and RPE cells were often multilayered to varying degrees, regardless of the molecular weight fraction in which they were cultured. Pink metachromatic toluidine blue staining between the RPE cells and the underlying ICL was found in some explants cultured in any of the three CM fractions (Fig. 6E).

Explants cultured in the 50-kDa filtrate had nuclear densities ranging from 22.1 to 42.7 nuclei/mm Bruch's membrane. With the exception of one explant, all were fully or almost fully resurfaced (i.e., small defects in the RPE coverage). Explants with the highest degree of resurfacing were resurfaced by RPE cells with islands of small, uniform cells (Figs. 4C, 4D, 5C, 5D). The expression of apical processes was highly variable and appeared to be related to cell size and shape (Figs. 4C, 5C, insets). RPE cells cultured in the 100-kDa filtrate had nuclear densities ranging from 16.2 to 30.0 nuclei/mm Bruch's membrane. The cells tended to be larger and flatter than cells cultured in the 50-kDa filtrate and unfiltered CM, with short apical processes when present (Figs. 5, 6). Five of 13 explants cultured in the 100-kDa filtrate were not fully resurfaced. RPE cultured in unfiltered CM had nuclear densities ranging from 21.1 to 39.2 nuclei/mm Bruch's membrane. RPE cell coverage of explants was complete or with small defects. Morphology was highly variable, ranging from small, flat cells to very large, flat cells.

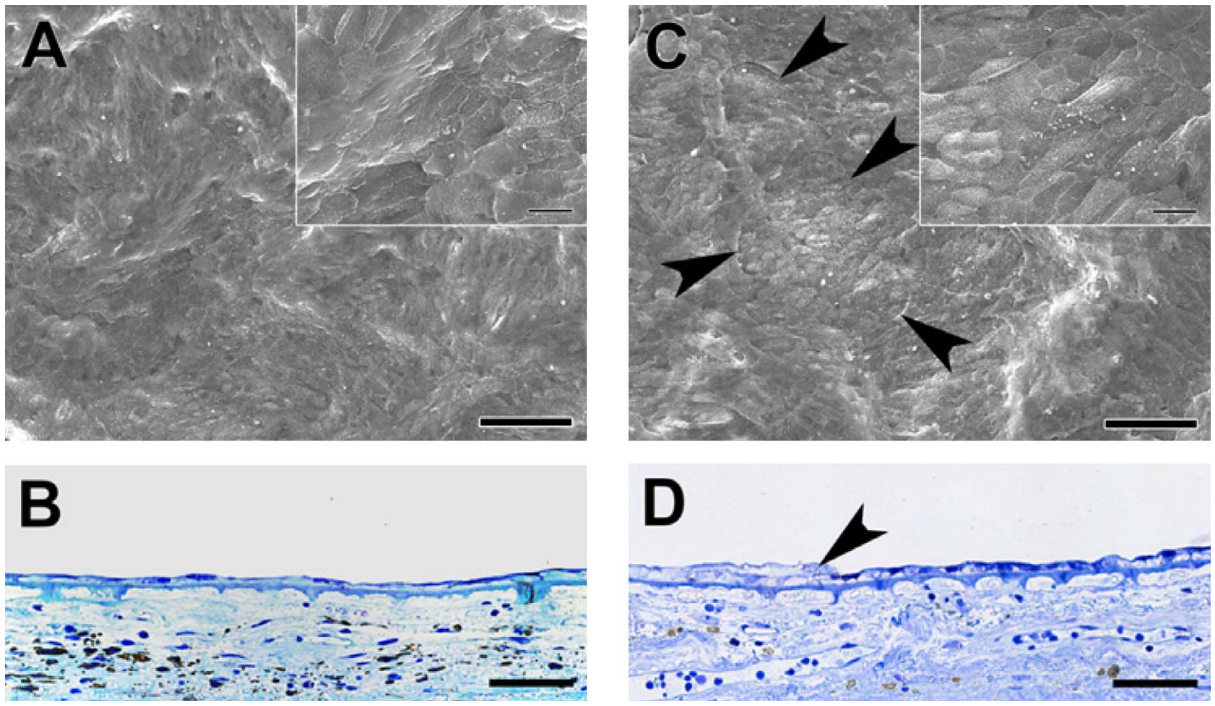

Figure 4. Comparison of RPE cell morphology after 21-day culture in 30- (A, B) and 50-kDa filtrates (C, D). (A) Predominantly large and flat RPE cells resurfaced half of the explant only. Cell surfaces were smooth with no or few short apical processes (*inset*). (B) RPE cells resurfacing the explant were mostly monolayered, large, and flat. The nuclear density was 17.65 ± 0.68 nuclei/mm Bruch's membrane. (C) RPE cells resurfacing the explant were largely multilayered with small defects in the RPE cell layer. Surface cells of the multilayer were large and flat. Small cells could be seen between areas of multilayering. *Arrowheads* point to the edge of a multilayer surrounding small cells. *High magnification inset* illustrates the variability in RPE cell size and the expression of apical processes on cell surfaces. (D) The explant was resurfaced by RPE cells that were highly variable in morphology. Although many cells were small, they were mainly flat (not columnar). *Arrowhead* points to the edge of a bilayer. The nuclear density was 37.44 ± 0.89 nuclei/mm Bruch's membrane. Donor was a 76-year-old Caucasian female with few submacular drusen in both eyes. (A, C) *magnification bar*, 100 μm; *inset bar* 20 μm. (B, D) *magnification bar* 50 μm, toluidine blue stained.

In summary, although extensive RPE resurfacing was observed in the 50-, 100-kDa filtrate, and unfiltered CM, the 50-kDa filtrate more uniformly supported RPE cell survival and differentiation on Bruch's membrane. The significantly higher nuclear density in the 50-kDa filtrate was associated with RPE cells that were smaller in size and appeared morphologically more mature than those observed in the 100-kDa filtrate and in unfiltered CM.

Combined Bioactive Fractions

The two bioactive fractions (<3-kDa filtrate and 10-50–kDa fraction) identified from testing CM subfractions were combined and used as medium to culture RPE cells on submacular human Bruch's membrane. RPE survival, based on nuclear density counts, was compared with survival after culture in the 50-kDa filtrate. The nuclear densities were not significantly different (Fig. 7), indicating that most of the bioactivity was found in the combined fractions. The ages of the two donor groups were not significantly different (Mann-Whitney Rank Sum test, $P = 0.767$).

In general, morphology after culture in the 50-kDa filtrate was better than that observed in the combined bioactive fractions. Although both culturing conditions can show variability in cell size and shape, large, flat RPE cells were more common after culture in the combined bioactive fractions (Fig. 8). One of five explants was not fully resurfaced after culture in the combined fractions.

RPE Survival in Cell Culture

The ability of CM fractions to support RPE cell attachment, proliferation, and survival was studied in cell culture on human collagen I (BD Bioscience), a major collagen component of the inner collagenous layer of Bruch's membrane.[10,11] RPE cell behavior in 3-kDa filtrate, 10-50–kDa fraction, and 50-kDa

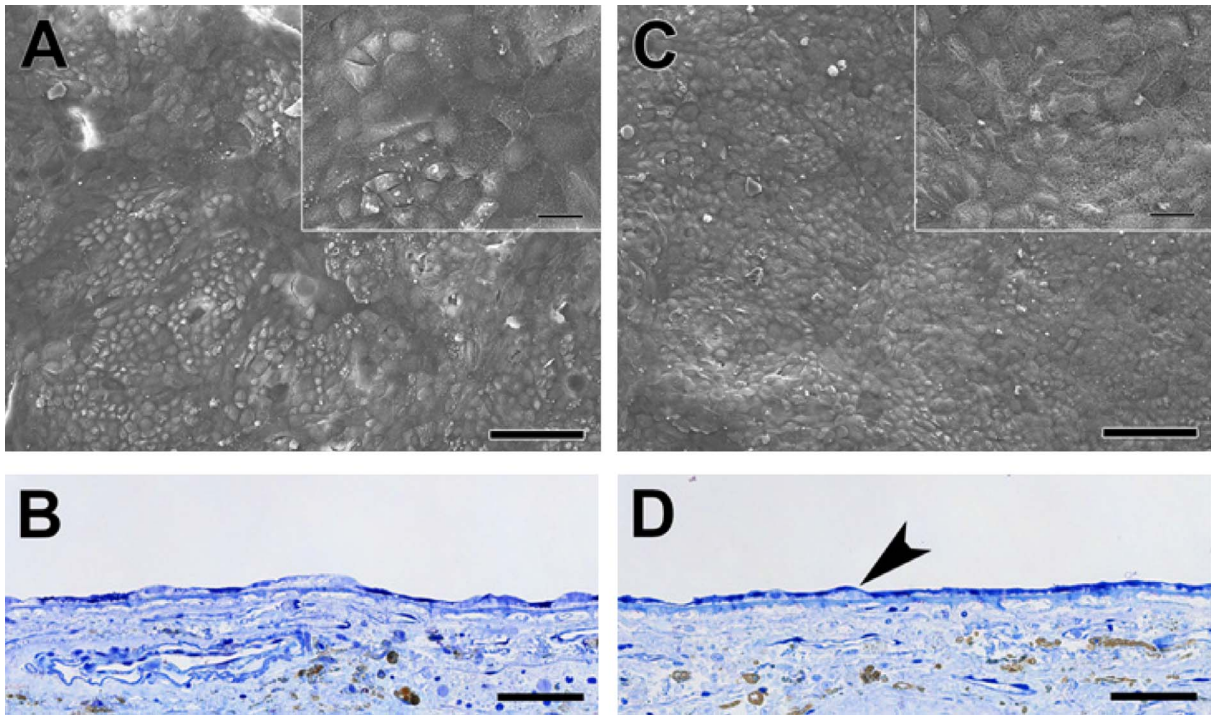

Figure 5. Comparison of RPE cell morphology after 21-day culture in 100- (A, B) and 50-kDa filtrates (C, D) on Bruch's membrane of an AMD donor. (A) The explant was extensively resurfaced by small cells surrounded by large flat cells. The variability of cell size is evident in the *inset*. When present, apical processes were short. (B) The variability in cell size was seen in tissue sections. Large ballooned cells were interspersed among small, flat cells. Nuclear density was 28.1 ± 0.36 nuclei/mm Bruch's membrane. (C) The explant was fully resurfaced by a fairly uniform layer of small RPE cells. Many cells were covered by well-developed apical processes (*inset*). (D) Tissue sections revealed that the cells were small and relatively flat. A thinned cell can be seen overlying a cell attached to Bruch's membrane (*arrowhead*). Nuclear density was 33.2 ± 0.44 nuclei/mm Bruch's membrane. Donor was an 81-year-old Caucasian female with choroidal new vessels in one eye (A, B) and abundant drusen in the fellow eye (C, D). (A, C) *magnification bar*, 100 μm; *inset bar* 20μm. (B, D) *magnification bar* 50 μm, toluidine blue stained.

filtrate from three different CM preparations was compared to RPE behavior in CM vehicle.

At day 1, there was some variability in the cultures in different CM fractions with some degree of spreading in all conditions. In two of three CM preparations, RPE cells were well spread and in confluent patches in the 3-kDa filtrate, in the 3-kDa filtrate +10-50–kDa fraction, and in the 50-kDa filtrate. RPE cells in the 10-50–kDa fraction and in CM vehicle were elongate with lamellipodia. In fractions from the remaining (third) CM preparation, RPE cells were elongate with lamellipodia in the 3-kDa filtrate and in the 10-50–kDa fraction, similar to RPE cells in CM vehicle. RPE cells in the 3-kDa filtrate +10-50–kDa fraction and in the 50-kDa filtrate also had elongate cells with lamellipodia, but also present were flattened cells in confluent patches. By day 3, RPE behavior was similar in fractions from all three of the CM preparations. RPE cells were confluent in the 3-kDa filtrate, in the 3-kDa filtrate +10-50–kDa fraction, and in the 50-kDa filtrate, but they were not confluent with elongate cells in the 10-50–kDa fraction and in CM vehicle. At day 7, RPE cells in the 3-kDa filtrate, in the 3-kDa filtrate +10-50–kDa fraction, and in the 50-kDa filtrate were confluent, small, and uniform in size. RPE cells in the 10-50–kDa fraction and in CM vehicle were rounded (dying). By day 14, only cellular debris remained in 10-50–kDa fraction and in CM vehicle cultures. The RPE cells in the 3-kDa filtrate, in the 3-kDa filtrate +10-50–kDa fraction, and in the 50-kDa filtrate continued to mature up to day 21, the longest time studied (Fig. 9).

The results of these experiments confirm the importance of the 3-kDa filtrate for CM bioactivity. Although the 3-kDa filtrate alone is not sufficient to support RPE cell survival (through day 21 in culture) and differentiation on aged and AMD Bruch's membrane, the 3-kDa filtrate alone contains mole-

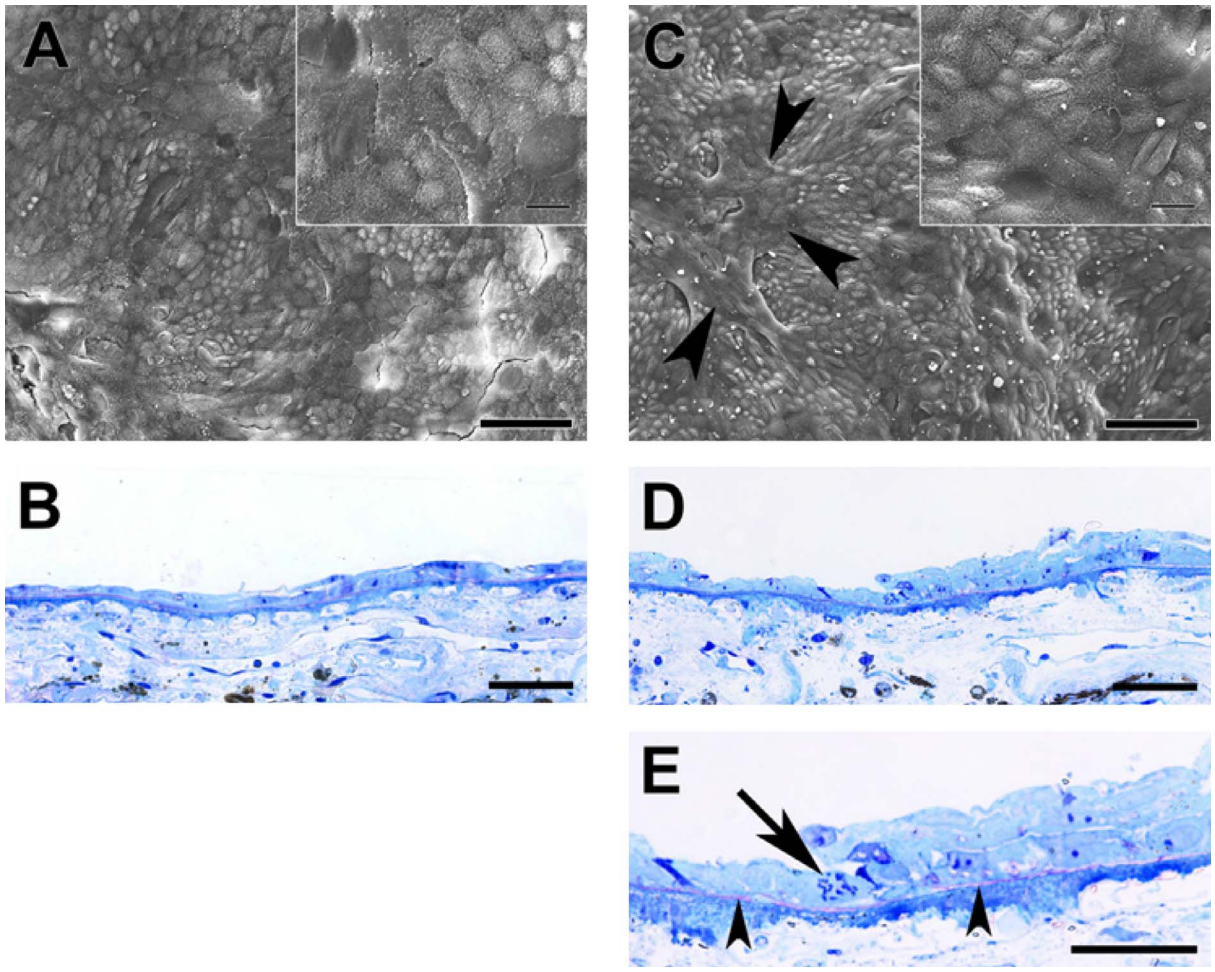

Figure 6. Comparison of RPE cell morphology after 21-day culture in 100-kDa filtrate (A, B) and unfiltered CM (C–E). (A) The explant was fully resurfaced with small defects in coverage by large, flat cells with localized areas of small cells. Apical processes, when present, were short (*inset*). (B) The explant was monolayered with localized areas of bilayering by thinned, very flat cells. The nuclear density was 23.2 ± 0.35 nuclei/mm Bruch's membrane. (C) This explant was fully resurfaced and heavily multilayered (*arrowheads* point to an area of thick multilayering). Apical processes were short to moderate in length (*inset*). (D) RPE cells resurfacing this explant were not as flattened as those seen on the fellow explant (B). Multilayering is evident in this section. (E) High magnification of the center of (D) shows pink metachromatic staining between the RPE cells and the surface of Bruch's membrane (*arrowheads*). *Arrow* points to a mitotic figure. Nuclear density was 25.5 ± 0.12 nuclei/mm Bruch's membrane. Donor was a 78-year-old Caucasian female with a few drusen in one eye (A, B) and no pathology in the fellow eye (C–E). (A, C) *magnification bar*, 100 μm; *inset magnification bar* 20 μm. (B, D) *magnification bar* 50 μm; (E) *magnification bar*, 30 μm, toluidine blue stained.

cules that can support RPE cell attachment and growth in culture on collagen I.

Mass Spectrometry of the Bioactive Fractions

Mass spectrometry of four different 10-50–kDa fractions from active CM identified 479 proteins found in at least three of four CM batches; 551 proteins were identified in at least three of four inactive CM (Table 1). These proteins were identified by database match to the IPI bovine database. Comparison of the putative protein composition of active versus inactive CM identified 50 proteins unique to active CM and 122 proteins unique to inactive CM. Table 1 is a summary of the number of proteins by location and function with the number of unique proteins in the last two columns.

Of the proteins identified in active CM, 175 proteins mapped to the extracellular space (Table 2). In addition to growth factors, cytokines, transporters, and peptidases, ECM molecules were identified in the function category "Other" (see Supplement Table S2 for full list of identified proteins in active CM).

Supplement Table S3 is a list of unique proteins found in active versus inactive 10-50–kDa CM.

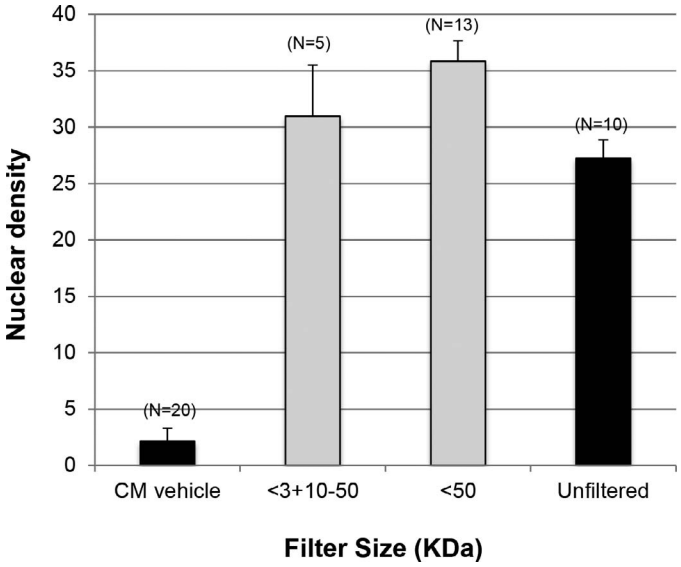

Figure 7. Nuclear density of RPE cells cultured in the combined bioactive fractions (3-kDa filtrate plus 10-50–kDa fraction, <3+10-50) compared with the nuclear density following culture in the 50-kDa filtrate (<50). Nuclear density of RPE cells after culture in the 50-kDa filtrate and the combined bioactive fractions were not significantly different ($P = 0.324$ Mann-Whitney Rank Sum Test). Nuclear densities of unfiltered CM and CM vehicle are included for reference.

Inactive CM contained significantly more intracellular (cytoplasmic and nuclear) proteins. Notable differences in growth factor composition were the presence of transforming growth factorβ–2 (TGFβ-2) and myostatin in active CM and hepatoma-derived growth factor in inactive CM.

Peptides representing protein fragments of 95 proteins were identified in at least two of three 3-kDa filtrates (not shown); 29 peptides were mapped to proteins unique to the 3-kDa fraction (i.e., protein not found in the 10-50–kDa fraction; Supplement Table S4).

CM Effects After Freeze/Thaw of Explants

In order to assess the possibility of choroidal cell contribution to RPE cell survival after culture in CM, additional explants were prepared to examine RPE survival on explants that were frozen and thawed prior to RPE cell seeding. Following explant preparation as described in Methods, one explant of a donor pair was frozen in liquid nitrogen and thawed at room temperature to kill live cells in the explant. After washing in DMEM, fetal RPE cells were seeded on explant pairs and cultured in 50-kDa CM filtrates for 21 days. RPE cells were able to resurface explants after freeze/thaw to the same degree as untreated explants (Fig. 10).

Discussion

In a previous study, we showed that culturing fetal RPE cells in CM greatly enhanced cell survival on aged human submacular Bruch's membrane, even in donor eyes with advanced AMD.[4] In the present study, as a first step in the identification of the bioactive molecules in CM, we performed size separation using commercially available filters of CM components to identify the fractions containing molecules contributing to enhanced RPE survival on aged and AMD submacular Bruch's membrane. Although we identified two bioactive fractions (i.e., <3-kDa filtrate and 10-50–kDa fraction), there was considerable variability in RPE nuclear density following culture in some of the fractions (i.e., 100-kDa retentate, 30-kDa filtrate, and 3-kDa filtrate + 10-50–kDa fraction). The variability may arise for several reasons. First, centrifugal filtration is not absolute; approximately 90% of a protein above the molecular size of the filter (nominal molecular weight limit, NMWL) is retained in the retentate (manufacturer specifications). Second, factors affecting variability in filtrate and retentate composition and protein/peptide concentration include molecular weight close to the NMWL, size, and shape of the molecule, and protein–protein interactions. Thus, filtration could result in variable amounts of a bioactive protein(s) present in the retentate or the filtrate, especially if that protein's size is close to the pore size of the filter or if the protein is bound to another molecule. Third, although we attempt to limit nonspecific binding by BSA coating of the filter, there is likely to be some nonspecific binding to the filter that could account for some loss of bioactivity, especially when a fraction is generated requiring two filtration steps (e.g., 10-50–kDa fraction). Thus, in addition to variability in RPE behavior that may be RPE or Bruch's membrane donor-specific, variability in fraction composition following size separation may contribute to variability in nuclear densities following culture in some of the fractions. Additional factors affecting CM fraction bioactivity might include biological variability in the composition of CM preparations (e.g., variability in protein concentrations) and changes in efficacy of the CM with storage. We have found that CM loses a significant amount of biological activity after 3-month storage at −80°C.

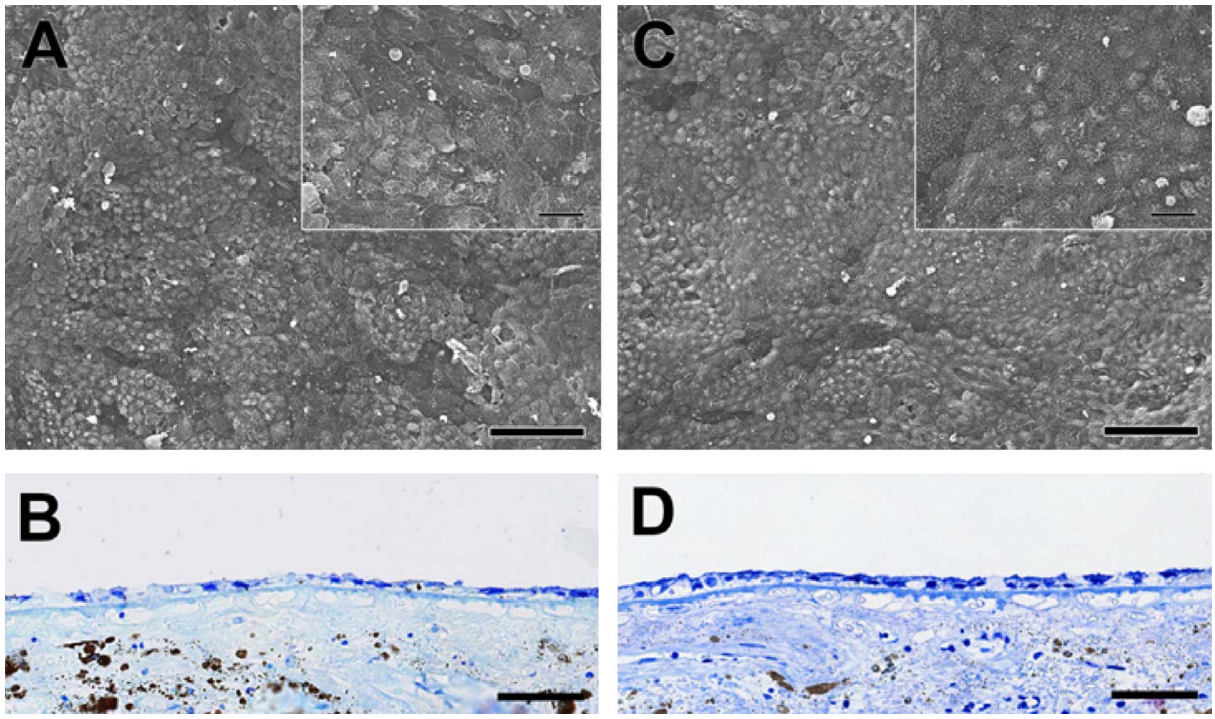

Figure 8. Comparison of RPE morphology after 21-day culture in combined bioactive fractions (3-kDa filtrate plus 10-50–kDa fraction; [A, B]) and 50-kDa filtrate (C, D). (A) Small defects in RPE resurfacing were found on this explant. Islands of small RPE were found between areas of large flat cells. The expression of apical processes was highly variable (*inset*). (B) RPE cells resurfacing Bruch's membrane were small but mostly flat. The variability in cellular morphology is evident in this section. Nuclear density of this explant was 40.0 ± 0.83 nuclei/mm Bruch's membrane. (C) RPE fully resurfaced this explant with a uniform layer of small cells with few areas of large, flattened cells. Cell surfaces were covered by apical processes (*inset*). (D) RPE resurfaced this explant more uniformly than the fellow explant (B). Small cells with lightly staining cytoplasm are found within the monolayer of smaller, compact cells. Nuclear density of this explant was 42.7 ± 1.14 nuclei/mm Bruch's membrane. The donor was a 68-year-old Middle Eastern female with no submacular pathology. (A, C) *magnification bar*, 100 μm; *inset bar* 20 μm. (B, D) *magnification bar* 50 μm, toluidine blue stained.

The removal of protein with filtration is significant. Unfiltered CM protein concentrations can range from 40 to 60 ug/ml; the protein concentration in the 100-kDa filtrate is approximately half that of unfiltered CM, and the 50-kDa filtrate has approximately 20-fold less protein than the 100-kDa filtrate. The increase in biological activity of the 50-kDa CM filtrate compared with both the unfiltered CM and the 100-kDa filtrate (Fig. 3) may signify the presence of an inhibitory or interference molecule (e.g., growth inhibitor, protease, cytotoxic substance, or other unidentified factor) that is lost or reduced with 50-kDa filtration. Further evidence for CM containing molecules that may be toxic to RPE cells can be seen by the comparison of protein components in active versus inactive CM (Table 1), where the presence of intracellular molecules in inactive CM is relatively high.

In testing the filtrates, removal of proteins above 10 kDa resulted in a significant drop in bioactivity, especially when compared with the activity of the 50-kDa filtrate. The RPE cell nuclear densities following culture in the 10-kDa filtrate were similar to those in CM vehicle (Fig. 3). The loss of bioactivity after removal of molecules following 10-kDa filtration, in addition to the high bioactivity of the 50-kDa filtrate, led us to conclude that the 10-50–kDa filtrate contains a significant fraction of CM bioactive molecules. Examination of proteins identified in the 10-50–kDa fraction by mass spectrometry (Table 2) that were mapped to the extracellular space (and therefore may function in extrinsic cell stimulation) discloses several functional categories that could contribute to the CM biological effect: growth factors and ECM molecules including ECM-associated molecules (found in Table 2 function category, "Other"). Growth factors are often added to basal culture medium to optimize cell growth, proliferation, and differentiation.[12,13] In some studies, identification of

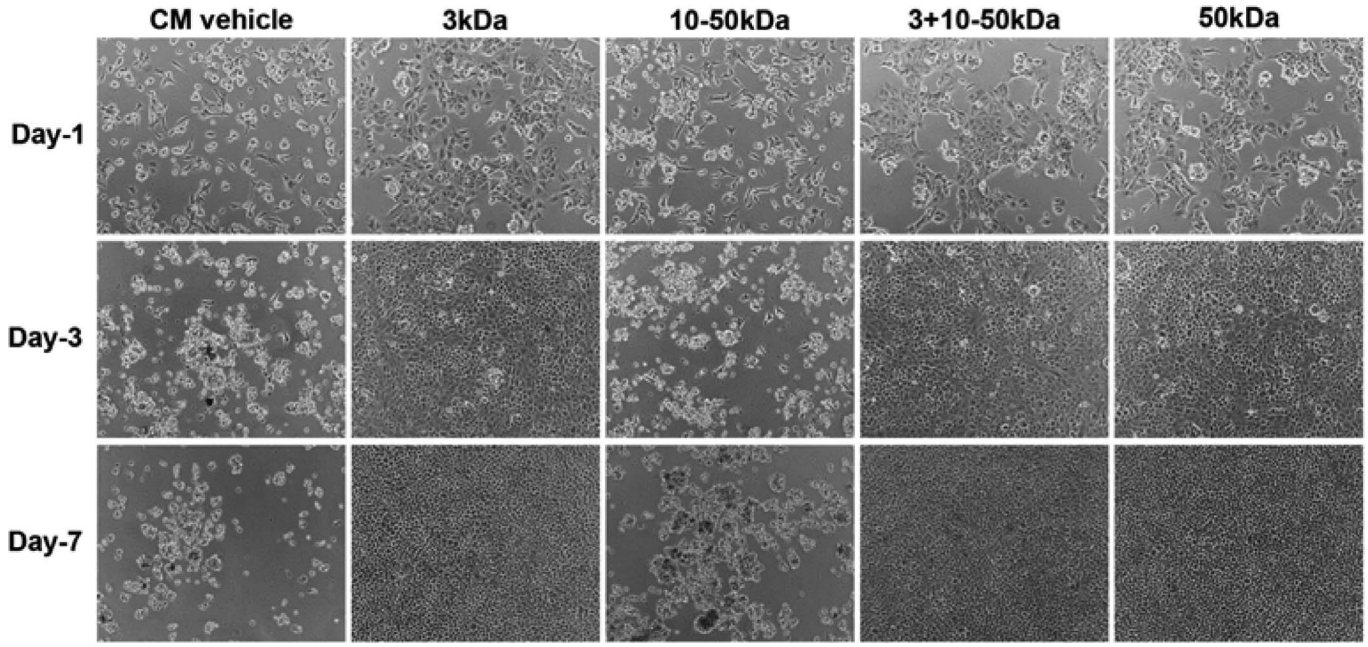

Figure 9. Behavior of fetal RPE in CM filtrates and CM vehicle on collagen I–coated tissue culture wells. The 3-kDa filtrate, 3-kDa filtrate +10-50–kDa fraction, and 50-kDa filtrate supported attachment, spreading, and proliferation of RPE with confluent cultures observed at day 3. Additional time in culture in these CM fractions resulted in confluent, small cells of uniform size. CM vehicle and the 10- to 50-kDa fraction supported limited attachment and spreading. By day-3, RPE in the latter culture conditions were dying. By day-7 only cellular debris was present.

which growth factor to add to culture media was based on those found in a conditioned medium.[14,15]

Of the 18 growth factors identified by mass spectrometry in the 10-50–kDa CM fraction, 12 growth factors could target RPE (Table 3). Connective tissue growth factor (CTGF) stimulates cell adhesion, proliferation, migration, and ECM formation in a variety of cell types. CTGF-stimulated collagen induction may require insulin or IGF, molecules that are found in bioactive CM fractions.[16] In addition to the full-length protein, CTGF fragments have bioactivity.[17] CTGF treatment increases RPE expression of ECM proteins including fibronectin, laminin, collagen I.[18–20] In our initial study examining the effects of CM on fetal RPE cells seeded onto tissue culture plastic and onto submacular Bruch's membrane, we showed CM exposure increases ECM deposition onto both substrates, compared with the amount of ECM deposition observed following culture in standard RPE medium.[4] The presence of proteoglycan staining (metachromatic toluidine blue staining, Fig. 6E) between the RPE and Bruch's membrane in some areas of explants showing a high degree of resurfacing suggests ECM deposition. Thus, CTGF could be a bioactive CM molecule, stimulating the observed increase in ECM deposition on Bruch's membrane. CTGF can act synergistically with TGFβ-2 in fetal RPE deposition of fibronectin containing extra domain A (FN-EDA).[21] TGFβ-2 alone also can stimulate ECM expression in RPE.[21–24]

Granulin is an epithelial cell mitogen that can be cleaved into 6-kDa peptides; these peptides can promote neuronal survival, cell migration, and inhibit or stimulate cell proliferation.[25] GAS6 is a protein that, when it activates the MER receptor of RPE, is thought to stimulate photoreceptor phagocytosis.[26,27] GAS6 has been shown to have survival and growth factor properties in other cell types.[28,29] Mimecan (truncated form of osteoglycin) can act synergistically with insulin-like growth factor-2 (IGF2), and insulin-like growth factor binding protein-2 (IGFBP2) to activate the IGF receptor, IGF1R, whose activation is associated with growth, survival, and differentiation.[30] Because fetal RPE cells were shown to express very little platelet-derived growth factor receptor-α (PDGFRα), the receptor activated by stimulation from PDGF-AA, PDGF-AA seems unlikely to be a bioactive molecule in CM.[31] PDGFRβ, activated by PDGF-AB, -BB, -CC (not found in CM), and -DD, is the major PDGF receptor found in fetal RPE. PDGF-AB, -BB, and -DD significantly enhance fetal RPE

Table 1. Comparison of the Protein Composition of the 10-50–kDa Fraction of Active Versus Inactive CM

Location	Function	Active	Inactive	Unique Active	Unique Inactive
Cytoplasm	Enzyme	74	82	12	20
	Kinase	5	5	0	0
	Growth factor	0	1	0	1
	Other	68	94	5	31
	Peptidase	18	19	0	1
	Phosphatase	1	4	0	3
	Transcription regulator	2	4	0	2
	Translation regulator	3	7	0	4
	Transporter	7	12	1	6
	Total	178	228	18	68
Extracellular space	Cytokine	12	12	0	0
	Enzyme	8	10	1	3
	Growth factor	18	17	2	1
	Other	103	102	8	6
	Peptidase	17	15	2	0
	Transporter	17	16	2	1
	Phosphatase	0	1	0	1
	Total	175	173	16	12
Nucleus	Enzyme	6	8	0	2
	Ion channel	0	1	0	1
	Other	19	26	2	9
	Peptidase	1	1	0	0
	Kinase	0	1	0	1
	Phosphatase	1	1	0	0
	Transcription regulator	5	10	0	5
	Translation regulator	1	1	0	0
	Total	33	49	2	18
Other	Enzyme	1	1	0	0
	Kinase	1	1	0	0
	Other	6	10	0	4
	Transporter	1	1	0	0
	Total	9	13	0	4
Plasma membrane	Enzyme	5	5	2	2
	G-protein coupled receptor	2	2	0	0
	Kinase	3	3	0	0
	Other	29	34	3	8
	Peptidase	5	5	0	0
	Transmembrane receptor	24	19	5	0
	Transporter	2	1	1	0
	Unknown	0	1	0	1
	Total	70	70	11	11
Unknown		14	19	4	9
	Total	479	551	50	122

Table 2. Proteins Identified in the Active 10-50–kDa Fraction That Mapped to the Extracellular Space

Protein	Molecular Weight	Gene	Location	Function
Chemokine (C-C motif) ligand 2	11 kDa	*CCL2*	Extracellular space	Cytokine
Chemokine (C-X-C motif) ligand 16	28 kDa	*CXCL16*	Extracellular space	Cytokine
Chemokine (C-X-C motif) ligand 2	11 kDa	*CXCL2*	Extracellular space	Cytokine
Chemokine (C-X-C motif) ligand 5	12 kDa	*CXCL5*	Extracellular space	Cytokine
Chromosome 19 open reading frame 10	19 kDa	*C19orf10*	Extracellular space	Cytokine
Colony stimulating factor 1 (macrophage)	60 kDa	*CSF1*	Extracellular space	Cytokine
Dickkopf WNT signaling pathway inhibitor 3	38 kDa	*DKK3*	Extracellular space	Cytokine
Family with sequence similarity 3, member C	25 kDa	*FAM3C*	Extracellular space	Cytokine
Macrophage migration inhibitory factor (glycosylation-inhibiting factor)	12 kDa	*MIF*	Extracellular space	Cytokine
Platelet factor 4	13 kDa	*PF4*	Extracellular space	Cytokine
Secreted phosphoprotein 1	31 kDa	*SPP1*	Extracellular space	Cytokine
TIMP metallopeptidase inhibitor 1	23 kDa	*TIMP1*	Extracellular space	Cytokine
Arylsulfatase family, member I	64 kDa	*ARSI*	Extracellular space	Enzyme
Calcium activated nucleotidase 1	45 kDa	*CANT1*	Extracellular space	Enzyme
Family with sequence similarity 20, member B	46 kDa	*FAM20B*	Extracellular space	Enzyme
Family with sequence similarity 20, member C	65 kDa	*FAM20C*	Extracellular space	Enzyme
Heparan sulfate proteoglycan 2	468 kDa	*HSPG2*	Extracellular space	Enzyme
Lysyl oxidase	47 kDa	*LOX*	Extracellular space	Enzyme
Lysyl oxidase-like 1	65 kDa	*LOXL1*	Extracellular space	Enzyme
Peroxidasin homolog (Drosophila)	158 kDa	*PXDN*	Extracellular space	Enzyme
Superoxide dismutase 3, extracellular	26 kDa	*SOD3*	Extracellular space	Enzyme
Bone morphogenetic protein 3	54 kDa	*BMP3*	Extracellular space	Growth factor
Connective tissue growth factor	38 kDa	*CTGF*	Extracellular space	Growth factor
C-type lectin domain family 11, member A	36 kDa	*CLEC11A*	Extracellular space	Growth factor
Endothelial cell-specific molecule 1	20 kDa	*ESM1*	Extracellular space	Growth factor
Granulin	63 kDa	*GRN*	Extracellular space	Growth factor
Growth arrest-specific 6	74 kDa	*GAS6*	Extracellular space	Growth factor
Insulin-like growth factor 1 (somatomedin C)	17 kDa	*IGF1*	Extracellular space	Growth factor
Insulin-like growth factor 2 (somatomedin A)	20 kDa	*IGF2*	Extracellular space	Growth factor
Myostatin	43 kDa	*MSTN*	Extracellular space	Growth factor
Neudesin neurotrophic factor	18 kDa	*NENF*	Extracellular space	Growth factor
Osteoglycin	34 kDa	*OGN*	Extracellular space	Growth factor
Platelet derived growth factor D	42 kDa	*PDGFD*	Extracellular space	Growth factor
Platelet-derived growth factor alpha polypeptide	24 kDa	*PDGFA*	Extracellular space	Growth factor
Platelet-derived growth factor beta polypeptide	27 kDa	*PDGFB*	Extracellular space	Growth factor
Transforming growth factor, beta 2	48 kDa	*TGFB2*	Extracellular space	Growth factor
Vascular endothelial growth factor A	22 kDa	*VEGFA*	Extracellular space	Growth factor
Vascular endothelial growth factor C	47 kDa	*VEGFC*	Extracellular space	Growth factor
VGF nerve growth factor inducible	68 kDa	*VGF*	Extracellular space	Growth factor
Adrenomedullin	21 kDa	*ADM*	Extracellular space	Other
Alpha-1-B glycoprotein	54 kDa	*A1BG*	Extracellular space	Other
Alpha-2-HS-glycoprotein	38 kDa	*AHSG*	Extracellular space	Other
Angiopoietin-like 7	39 kDa	*ANGPTL7*	Extracellular space	Other
Biglycan	42 kDa	*BGN*	Extracellular space	Other

Table 2. Continued

Protein	Molecular Weight	Gene	Location	Function
Chitinase domain containing 1	45 kDa	*CHID1*	Extracellular space	Other
Chordin	102 kDa	*CHRD*	Extracellular space	Other
Cofilin 2 (muscle)	19 kDa	*CFL2*	Extracellular space	Other
Collagen triple helix repeat containing 1	26 kDa	*CTHRC1*	Extracellular space	Other
Collagen, type I, alpha 2	129 kDa	*COL1A2*	Extracellular space	Other
Collagen, type III, alpha 1	138 kDa	*COL3A1*	Extracellular space	Other
Collagen, type IV, alpha 1	160 kDa	*COL4A1*	Extracellular space	Other
Collagen, type IV, alpha 2	165 kDa	*COL4A2*	Extracellular space	Other
Collagen, type V, alpha 2	30 kDa	*COL5A2*	Extracellular space	Other
Collagen, type VI, alpha 1	109 kDa	*COL6A1*	Extracellular space	Other
Collagen, type VI, alpha 2	109 kDa	*COL6A2*	Extracellular space	Other
Collagen, type VIII, alpha 1	73 kDa	*COL8A1*	Extracellular space	Other
Collagen, type VIII, alpha 2	67 kDa	*COL8A2*	Extracellular space	Other
Collagen, type XI, alpha 1	182 kDa	*COL11A1*	Extracellular space	Other
Collagen, type XII, alpha 1	340 kDa	*COL12A1*	Extracellular space	Other
Collagen, type XVI, alpha 1	160 kDa	*COL16A1*	Extracellular space	Other
Complement component 4B (Chido blood group)	193 kDa	*C4A*	Extracellular space	Other
Complement factor H	140 kDa	*CFH*	Extracellular space	Other
Complement factor H-related 1	65 kDa	*CFHR1*	Extracellular space	Other
Cystatin C	16 kDa	*CST3*	Extracellular space	Other
Cystatin E/M	16 kDa	*CST6*	Extracellular space	Other
Cysteine-rich, angiogenic inducer, 61	42 kDa	*CYR61*	Extracellular space	Other
Decorin	40 kDa	*DCN*	Extracellular space	Other
Dickkopf WNT signaling pathway inhibitor 2	28 kDa	*DKK2*	Extracellular space	Other
Dickkopf-like 1	26 kDa	*DKKL1*	Extracellular space	Other
EGF containing fibulin-like extracellular matrix protein 1	55 kDa	*EFEMP1*	Extracellular space	Other
EGF containing fibulin-like extracellular matrix protein 2	50 kDa	*EFEMP2*	Extracellular space	Other
Elastin microfibril interfacer 1	107 kDa	*EMILIN1*	Extracellular space	Other
Fetuin B	43 kDa	*FETUB*	Extracellular space	Other
Fibrillin 1	313 kDa	*FBN1*	Extracellular space	Other
Fibrinogen alpha chain	67 kDa	*FGA*	Extracellular space	Other
Fibromodulin	43 kDa	*FMOD*	Extracellular space	Other
Fibulin 1	78 kDa	*FBLN1*	Extracellular space	Other
Fibulin 5	50 kDa	*FBLN5*	Extracellular space	Other
Follistatin	38 kDa	*FST*	Extracellular space	Other
Follistatin-like 1	35 kDa	*FSTL1*	Extracellular space	Other
Follistatin-like 3 (secreted glycoprotein)	28 kDa	*FSTL3*	Extracellular space	Other
Galanin/GMAP prepropeptide	13 kDa	*GAL*	Extracellular space	Other
Gelsolin	86 kDa	*GSN*	Extracellular space	Other
Histidine-rich glycoprotein	62 kDa	*HRG*	Extracellular space	Other
Hyaluronan and proteoglycan link protein 3	41 kDa	*HAPLN3*	Extracellular space	Other

Table 2. Continued

Protein	Molecular Weight	Gene	Location	Function
Immunoglobulin J polypeptide, linker protein for immunoglobulin alpha and mu polypeptides	18 kDa	*IGJ*	Extracellular space	Other
Insulin	11 kDa	*INS*	Extracellular space	Other
Insulin-like growth factor binding protein 2, 36kda	34 kDa	*IGFBP2*	Extracellular space	Other
Insulin-like growth factor binding protein 3	262 kDa	*IGFBP3*	Extracellular space	Other
Insulin-like growth factor binding protein 4	28 kDa	*IGFBP4*	Extracellular space	Other
Insulin-like growth factor binding protein 5	30 kDa	*IGFBP5*	Extracellular space	Other
Insulin-like growth factor binding protein 6	25 kDa	*IGFBP6*	Extracellular space	Other
Insulin-like growth factor binding protein, acid labile subunit	66 kDa	*IGFALS*	Extracellular space	Other
Inter-alpha-trypsin inhibitor heavy chain 2	106 kDa	*ITIH2*	Extracellular space	Other
Inter-alpha-trypsin inhibitor heavy chain family, member 4	102 kDa	*ITIH4*	Extracellular space	Other
Kininogen 1	69 kDa	*KNG1*	Extracellular space	Other
Laminin, beta 1	197 kDa	*LAMB1*	Extracellular space	Other
Latent transforming growth factor beta binding protein 2	212 kDa	*LTBP2*	Extracellular space	Other
Latent transforming growth factor beta binding protein 3	139 kDa	*LTBP3*	Extracellular space	Other
Lectin, galactoside-binding, soluble, 1	15 kDa	*LGALS1*	Extracellular space	Other
Lectin, galactoside-binding, soluble, 3	28 kDa	*LGALS3*	Extracellular space	Other
Lumican	39 kDa	*LUM*	Extracellular space	Other
Matrix Gla protein	12 kDa	*MGP*	Extracellular space	Other
Melanoma inhibitory activity	14 kDa	*MIA*	Extracellular space	Other
Mesothelin	44 kDa	*MSLN*	Extracellular space	Other
Meteorin, glial cell differentiation regulator	31 kDa	*METRN*	Extracellular space	Other
Microfibrillar-associated protein 2	21 kDa	*MFAP2*	Extracellular space	Other
Microfibrillar-associated protein 4	29 kDa	*MFAP4*	Extracellular space	Other
Nidogen 1	136 kDa	*NID1*	Extracellular space	Other
Niemann-Pick disease, type C2	17 kDa	*NPC2*	Extracellular space	Other
Olfactomedin-like 3	46 kDa	*OLFML3*	Extracellular space	Other
Orosomucoid 1	23 kDa	*ORM1*	Extracellular space	Other
Periostin, osteoblast specific factor	93 kDa	*POSTN*	Extracellular space	Other
Plexin domain containing 2	59 kDa	*PLXDC2*	Extracellular space	Other
Procollagen C-endopeptidase enhancer	48 kDa	*PCOLCE*	Extracellular space	Other
Proline/arginine-rich end leucine-rich repeat protein	44 kDa	*PRELP*	Extracellular space	Other
Proprotein convertase subtilisin/kexin type 1 inhibitor	27 kDa	*PCSK1N*	Extracellular space	Other
Prosaposin	58 kDa	*PSAP*	Extracellular space	Other
Protein S (alpha)	75 kDa	*PROS1*	Extracellular space	Other
Secreted protein, acidic, cysteine-rich (osteonectin)	35 kDa	*SPARC*	Extracellular space	Other
Secretogranin V (7B2 protein)	24 kDa	*SCG5*	Extracellular space	Other

Table 2. Continued

Protein	Molecular Weight	Gene	Location	Function
Sema domain, immunoglobulin domain (Ig), short basic domain, secreted, (semaphorin) 3C	85 kDa	*SEMA3C*	Extracellular space	Other
Serpin peptidase inhibitor, clade A (alpha-1 antiproteinase, antitrypsin), member 3	46 kDa	*SERPINA3*	Extracellular space	Other
Serpin peptidase inhibitor, clade E (nexin, plasminogen activator inhibitor type 1), member 1	45 kDa	*SERPINE1*	Extracellular space	Other
Serpin peptidase inhibitor, clade E (nexin, plasminogen activator inhibitor type 1), member 2	44 kDa	*SERPINE2*	Extracellular space	Other
Serpin peptidase inhibitor, clade F (alpha-2 antiplasmin, pigment epithelium derived factor), member 1	46 kDa	*SERPINF1*	Extracellular space	Other
Serpin peptidase inhibitor, clade G (C1 inhibitor), member 1	52 kDa	*SERPING1*	Extracellular space	Other
Serpin peptidase inhibitor, clade H (heat shock protein 47), member 1, (collagen binding protein 1)	47 kDa	*SERPINH1*	Extracellular space	Other
Sex hormone-binding globulin	43 kDa	*SHBG*	Extracellular space	Other
Slit homolog 3 (Drosophila)	171 kDa	*SLIT3*	Extracellular space	Other
Somatomedin B and thrombospondin, type 1 domain containing	29 kDa	*SBSPON*	Extracellular space	Other
SPARC related modular calcium binding 1	48 kDa	*SMOC1*	Extracellular space	Other
Spondin 1, extracellular matrix protein	91 kDa	*SPON1*	Extracellular space	Other
Thrombospondin 1	130 kDa	*THBS1*	Extracellular space	Other
Thrombospondin 4	106 kDa	*THBS4*	Extracellular space	Other
TIMP metallopeptidase inhibitor 2	24 kDa	*TIMP2*	Extracellular space	Other
Tsukushi, small leucine rich proteoglycan	37 kDa	*TSKU*	Extracellular space	Other
Twisted gastrulation BMP signaling modulator 1	25 kDa	*TWSG1*	Extracellular space	Other
Ubiquinol-cytochrome c reductase complex assembly factor 3	10 kDa	*UQCC3*	Extracellular space	Other
Vitronectin	54 kDa	*VTN*	Extracellular space	Other
WD repeat domain 1	66 kDa	*WDR1*	Extracellular space	Other
ADAM metallopeptidase with thrombospondin type 1 motif, 1	105 kDa	*ADAMTS1*	Extracellular space	Peptidase
ADAM metallopeptidase with thrombospondin type 1 motif, 3	136 kDa	*ADAMTS3*	Extracellular space	Peptidase
ADAM metallopeptidase with thrombospondin type 1 motif, 5	102 kDa	*ADAMTS5*	Extracellular space	Peptidase
Coagulation factor II (thrombin)	71 kDa	*F2*	Extracellular space	Peptidase
Complement component 1, r subcomponent	80 kDa	*C1R*	Extracellular space	Peptidase
Complement component 1, s subcomponent	77 kDa	*C1S*	Extracellular space	Peptidase
Complement component 2	83 kDa	*C2*	Extracellular space	Peptidase
Complement component 3	187 kDa	*C3*	Extracellular space	Peptidase
Complement factor B	85 kDa	*CFB*	Extracellular space	Peptidase

Table 2. Continued

Protein	Molecular Weight	Gene	Location	Function
HtrA serine peptidase 1	67 kDa	*HTRA1*	Extracellular space	Peptidase
Matrix metallopeptidase 14 (membrane-inserted)	66 kDa	*MMP14*	Extracellular space	Peptidase
Matrix metallopeptidase 16 (membrane-inserted)	69 kDa	*MMP16*	Extracellular space	Peptidase
Matrix metallopeptidase 2 (gelatinase A, 72 kda gelatinase, 72 kda type IV collagenase)	74 kDa	*MMP2*	Extracellular space	Peptidase
Matrix metallopeptidase 3 (stromelysin 1, progelatinase)	54 kDa	*MMP3*	Extracellular space	Peptidase
Plasminogen	91 kDa	*PLG*	Extracellular space	Peptidase
Protease, serine, 23	42 kDa	*PRSS23*	Extracellular space	Peptidase
Protease, serine, 35	47 kDa	*PRSS35*	Extracellular space	Peptidase
Albumin	69 kDa	*ALB*	Extracellular space	Transporter
Alpha-2-macroglobulin	168 kDa	*A2M*	Extracellular space	Transporter
Alpha-fetoprotein	69 kDa	*AFP*	Extracellular space	Transporter
Apolipoprotein A-I	30 kDa	*APOA1*	Extracellular space	Transporter
Apolipoprotein A-II	11 kDa	*APOA2*	Extracellular space	Transporter
Apolipoprotein A-IV	43 kDa	*APOA4*	Extracellular space	Transporter
Apolipoprotein C-III	11 kDa	*APOC3*	Extracellular space	Transporter
Apolipoprotein D	24 kDa	*APOD*	Extracellular space	Transporter
Apolipoprotein E	36 kDa	*APOE*	Extracellular space	Transporter
Apolipoprotein H (beta-2-glycoprotein I)	38 kDa	*APOH*	Extracellular space	Transporter
Hemoglobin subunit alpha	15 kDa	*HBA1*	Extracellular space	Transporter
Hemopexin	52 kDa	*HPX*	Extracellular space	Transporter
Insulin-like growth factor binding protein 7	29 kDa	*IGFBP7*	Extracellular space	Transporter
Retinol binding protein 1, cellular	16 kDa	*RBP1*	Extracellular space	Transporter
Retinol binding protein 4, plasma	23 kDa	*RBP4*	Extracellular space	Transporter
Transferrin	78 kDa	*TF*	Extracellular space	Transporter
Transthyretin	16 kDa	*TTR*	Extracellular space	Transporter

proliferation and migration with PDGF-DD showing a greater stimulatory ability than PDGF-AB and -BB.[31] A study by Nagineni et al.[32] reported no enhanced RPE proliferation (donor age unknown) from PDGFAA, AB, and BB. PDGF can act synergistically with IGF-1 and insulin (mapped to extracellular space, other in Table 2), stimulating RPE proliferation.[33] IGF-1 and IGF-2 can be used singly to stimulate proliferation of RPE cells.[34–36] Insulin (which can also activate the IGF receptor) is used routinely in cell culture medium to promote cell survival and proliferation[37] and is a supplement of MDBK-MM (CM vehicle). However, insulin alone cannot be attributed to CM bioactivity since MDBK-MM does not support RPE cell survival on Bruch's membrane. Vascular endothelial growth factors (VEGFs) are angiogenic factors that primarily target endothelial cells.[38,39] VEGFA can compromise RPE barrier function resulting in a reduction of transepithelial resistance.[40,41] However, VEGFA has also been shown to be a RPE cell survival factor under conditions of oxidative stress.[42,43] VEGF can stimulate RPE cell proliferation but, when combined with IGF-1, decreases proliferation over that seen by these growth factors applied singly.[44] Thus, it seems plausible that some or all of the above growth factors with or without insulin could be bioactive in CM, stimulating proliferation, ECM deposition, and enhanced RPE cell survival on submacular Bruch's membrane.

We compared the protein composition of active versus inactive CM to determine whether there were qualitative differences that could account for activity.

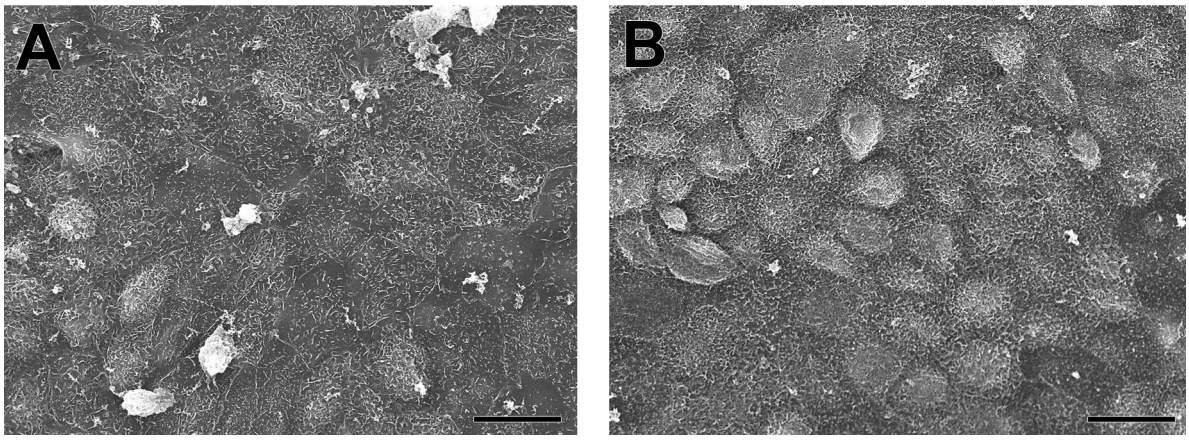

Figure 10. Behavior of fetal RPE on Bruch's membrane after freeze/thaw and CM culture. RPE were able to resurface Bruch's membrane after explant freeze/thaw (A) in a manner similar to the fellow explant that had not been subject to a freeze/thaw cycle. (B) The donor was a 79-year-old Caucasian female, no submacular pathology. *Magnification bar*, 20 μm.

Two growth factors were present in active CM that were lacking in inactive CM, myostatin (target cell, muscle), and TGFβ-2 (Supplement Table S3A). In addition to ECM expression/deposition, TGFβ-2 can also stimulate epithelial to mesenchymal transition[45] and can reduce proliferation potential.[24,46] TGFβ-2 combined with growth factors found in CM (IGF-1, VEGF, PDGF) reduced the proliferation potential of the single growth factors when applied to RPE in culture.[44] Thus, lack of TGFβ-2 in inactive CM might account for inactivity if increased ECM deposition underlies enhanced RPE survival on aged/AMD Bruch's membrane. However, increased ECM deposition after CM culture compared with ECM deposition in RPE medium could also be a consequence of enhanced long-term survival after CM culture. The most striking difference in the composition of the two preparations was the greater presence of intracellular proteins found in inactive CM. Therefore, inactive CM could be inactive due to the presence of toxic

Table 3. Target Cells of Growth Factors Identified in 10-50–kDa CM

Protein	Gene	Target Cell*
Bone morphogenetic protein 3	*BMP3*	Bone
Connective tissue growth factor	*CTGF*	RPE
C-type lectin domain family 11, member A	*CLEC11A*	Hemapoetic cells
Endothelial cell-specific molecule 1	*ESM1*	Endothelial cells
Granulin	*GRN*	Epithelial cells
Growth arrest-specific 6	*GAS6*	RPE
Insulin-like growth factor 1 (somatomedin C)	*IGF1*	RPE
Insulin-like growth factor 2 (somatomedin A)	*IGF2*	RPE
Myostatin	*MSTN*	Muscle
Neudesin neurotrophic factor	*NENF*	Neurons
Osteoglycin	*OGN*	Bone, other cell types (mimecan)
Platelet derived growth factor D	*PDGFD*	RPE
Platelet-derived growth factor alpha polypeptide	*PDGFA*	Nonfetal RPE (PDGFAA)
Platelet-derived growth factor beta polypeptide	*PDGFB*	RPE
Transforming growth factor, beta 2	*TGFB2*	RPE
Vascular endothelial growth factor A	*VEGFA*	RPE
Vascular endothelial growth factor C	*VEGFC*	RPE
VGF nerve growth factor inducible	*VGF*	Neurons

* Information for non-RPE target cells is from genecards.com. See text for RPE target cell references.

intracellular molecules, released by dead/dying BCE during CM manufacture.

Fragments of several ECM proteins are present in the 10-50–kDa fraction: subunits for collagens and the glycoproteins nidogen 1, fibulin, thrombospondin, thrombospondin, and laminin. Most of these proteins have molecular weight well above 50-kDa, indicating that these ECM molecules are likely to be present as protein fragments or peptides in the 50-kDa filtrate. Peptides or fragments of some of these molecules are capable of cell stimulation that could lead to enhanced cell proliferation or survival.[47–49] Also present in the CM 10-50–kDa fraction are small leucine-rich proteoglycans (SLRPs) involved in ECM assembly (e.g., decorin, fibromodulin, and lumican).[50] Proteoglycans (e.g., HSPG2, ESM-1, and SLRPs) can play a role in adhesion, migration, proliferation, and survival through binding and delivery or sequestration of growth factors and interaction with ECM components.[37,51,52] Although HSPG2 (perlecan) has a molecular weight well above the filter size (468 kDa), fragments of HSPG2 support adhesion and spreading and growth factor delivery.[53–55]

Testing retentates above the NMWL of the filters revealed a necessary low molecular weight bioactive CM component of approximate molecular weight 3 kDa or less. Medium supplements of low molecular weight in CM vehicle such as insulin, hydrocortisone, selenium, amino acids, and vitamins are not sufficient, however, as the retentate fractions are reconstituted to original volume by CM vehicle for testing in the Bruch's membrane assay, and CM vehicle alone does not support cell survival on Bruch's membrane or on collagen I–coated tissue culture wells (Figs. 1 and 9). Thus, inability of retentate fractions to support RPE on Bruch's membrane indicates that molecules not present in the basal medium (CM vehicle) and present in 3-kDa filtrate are contributing to the biological effect.

Although the 3-kDa filtrate alone did not support RPE cell survival on submacular Bruch's membrane, the 3-kDa filtrate was sufficient to support RPE cells on collagen I–coated tissue culture wells (Fig. 9). These results, in addition to the poor support of RPE cells in retentates and in CM vehicle alone, are consistent with the notion that the 3-kDa filtrate contains additional beneficial molecules that are not present or are not present in sufficient quantities in the CM vehicle. Poor RPE cell survival on Bruch's membrane after culture in 3-kDa filtrate is similar to that seen after organ culture in RPE medium, which also supports rapid RPE cell attachment and growth in cell culture. RPE medium includes basic fibroblast growth factor (bFGF) and fetal bovine serum, which contains growth factors, ECM components, vitamins, hormones, and trace elements.[56] Because the 3-kDa filtrate is sufficient to support growth and maturity of RPE cells in cell culture, the 10-50–kDa fraction may provide survival factors to prevent RPE death on Bruch's membrane. These survival factors may not be present in RPE medium.

Peptide analysis of the 3-kDa filtrate identified mainly protein fragments of proteins that were found in the 10-50–kDa fraction (Supplement Table S4). Peptides of seven proteins mapping to the extracellular space were identified that were not found in the 10-50–kDa fraction. However, these peptides are from proteins that are unlikely to have stimulatory effects on RPE. It is possible that molecules other than peptides (e.g., lipid signaling molecules) could contribute to 3-kDa filtrate activity.

The studies examining RPE cell behavior on explants that have been subject to liquid nitrogen freezing and rapid thaw, point to the transplanted RPE as the CM target cell. Examination of explant sections by light microscopy in previous studies showed that in many explants, particularly those from AMD donors, the choriocapillaris is degenerating or degenerated,[5,6] eliminating the contribution of choriocapillaris endothelial cells to enhanced RPE survival on Bruch's membrane. These observations and the results from killing explant cells by freeze/thaw prior to RPE transplantation indicate that RPE are likely the CM target cell.

In summary, we have identified two CM bioactive fractions that support RPE cell survival on AMD Bruch's membrane: a 10-50–kDa fraction that includes several growth factors and other proteins that could act as cofactors, and a less than 3-kDa fraction that is not likely to have an active peptide/protein fragment component. Analysis of the 10-50–kDa fraction demonstrates the presence of several molecules that may be intact in CM or that have been shown to have active soluble fragments or peptides capable of stimulating RPE cell growth and survival. The results of this study represent an initial step in the identification of molecules that support RPE cell survival and differentiation on aged and AMD submacular Bruch's membrane. The long-term goal of these studies is to identify bioactive CM molecules that can be used clinically to improve the efficacy of cell transplants in patients with advanced AMD.

Acknowledgments

The authors wish to thank Dr. Celia Nunes and Ms. Aprille Rapista for technical assistance and Ms. Ashley Morganti and Mr. Nicholas Sprehe of the Lions Institute for Transplant and Research for facilitation of donor eye acquisition.

Supported by grants from the Foundation Fighting Blindness, the Lincy Foundation, an unrestricted grant from Research to Prevent Blindness, the Eye Institute of New Jersey, the Janice Mitchell Vassar and Ashby John Mitchell Fellowship, the Joseph J. and Marguerite DiSepio Retina Research Fund, the Eng Family Fund for Excellence in Ophthalmology, the New Jersey Healthcare Foundation, the William L. Seery Endowment Fund, the Alfonse A. Cinotti, M.D./Lions Eye Research Chair, and the New Jersey Lions Eye Research Foundation. The mass spectrometry study was funded in part by National Institutes of Health Grant NS046593 to the Neuroproteomics Core Facility (HL).

Disclosure: **I.K. Sugino,** P; **Q. Sun,** P; **C. Springer,** None; **N Cheewatrakoolpong,** None; **T. Liu,** None; **H. Li,** None; **M.A. Zarbin,** P, C, R, S

References

1. Bharti K, Rao M, Hull SC, et al. Developing cellular therapies for retinal degenerative diseases. *Invest Ophthalmol Vis Sci*. 2014;55:1191–1202.
2. Schwartz SD, Regillo CD, Lam BL, et al. Human embryonic stem cell-derived retinal pigment epithelium in patients with age-related macular degeneration and Stargardt's macular dystrophy: follow-up of two open-label phase 1/2 studies. *Lancet*. 2015;385:509–516.
3. Song WK, Park KM, Kim HJ, et al. Treatment of macular degeneration using embryonic stem cell-derived retinal pigment epithelium: preliminary results in Asian patients. *Stem Cell Reports*. 2015; 4:860–872.
4. Sugino IK, Rapista A, Sun Q, et al. A method to enhance cell survival on Bruch's membrane in eyes affected by age and age-related macular degeneration. *Invest Ophthalmol Vis Sci*. 2011;52: 9598–9609.
5. Sugino IK, Gullapalli VK, Sun Q, et al. Cell-deposited matrix improves retinal pigment epithelium survival on aged submacular human Bruch's membrane. *Invest Ophthalmol Vis Sci*. 2011;52:1345–1358.
6. Sugino IK, Sun Q, Wang J, et al. Comparison of FRPE and human embryonic stem cell-derived RPE behavior on aged human Bruch's membrane. *Invest Ophthalmol Vis Sci*. 2011;52:4979–4997.
7. Zarbin MA. Analysis of retinal pigment epithelium integrin expression and adhesion to aged submacular human Bruch's membrane. *Trans Am Ophthalmol Soc*. 2003;101:499–520.
8. Gullapalli VK, Sugino IK, Van Patten Y, Shah S, Zarbin MA. Retinal pigment epithelium resurfacing of aged submacular human Bruch's membrane. *Trans Am Ophthalmol Soc*. 2004;102:123–137, discussion 137–128.
9. Gullapalli VG. *Paucity of cellular integrin receptors and aging changes in Bruch's membrane contribute to poor resurfacing of aged Bruch's membrane by retinal pigment epithelium*. Newark, NJ: Graduate School of Biomedical Sciences: 2005. Thesis.
10. Das A, Frank RN, Zhang NL, Turczyn TJ. Ultrastructural localization of extracellular matrix components in human retinal vessels and Bruch's membrane. *Arch Ophthalmol*. 1990;108: 421–429.
11. Marshall GE, Konstas AG, Reid GG, Edwards JG, Lee WR. Collagens in the aged human macula. *Graefe's Arch Clin Exp Ophthalmol*. 1994;232:133–140.
12. Vater C, Kasten P, Stiehler M. Culture media for the differentiation of mesenchymal stromal cells. *Acta Biomater*. 2011;7:463–477.
13. Jung S, Panchalingam KM, Rosenberg L, Behie LA. Ex vivo expansion of human mesenchymal stem cells in defined serum-free media. *Stem Cells Int*. 2012;2012:123030.
14. Lim UM, Yap MG, Lim YP, Goh LT, Ng SK. Identification of autocrine growth factors secreted by CHO cells for applications in single-cell cloning media. *J Proteome Res*. 2013;12:3496–3510.
15. Hauck SM, Gloeckner CJ, Harley ME, et al. Identification of paracrine neuroprotective candidate proteins by a functional assay-driven proteomics approach. *Mol Cell Proteomics*. 2008;7:1349–1361.
16. Lipson KE, Wong C, Teng Y, Spong S. CTGF is a central mediator of tissue remodeling and fibrosis and its inhibition can reverse the process of fibrosis. *Fibrogenesis Tissue Repair*. 2012;5:S24.
17. de Winter P, Leoni P, Abraham D. Connective tissue growth factor: structure-function relation-

ships of a mosaic, multifunctional protein. *Growth Factors*. 2008;26:80–91.
18. Zhu J, Nguyen D, Ouyang H, Zhang XH, Chen XM, Zhang K. Inhibition of RhoA/Rho-kinase pathway suppresses the expression of extracellular matrix induced by CTGF or TGF-beta in ARPE-19. *Int J Ophthalmol*. 2013;6:8–14.
19. Nagai N, Klimava A, Lee WH, Izumi-Nagai K, Handa JT. CTGF is increased in basal deposits and regulates matrix production through the ERK (p42/p44mapk) MAPK and the p38 MAPK signaling pathways. *Invest Ophthalmol Vis Sci*. 2009;50:1903–1910.
20. He S, Chen Y, Khankan R, et al. Connective tissue growth factor as a mediator of intraocular fibrosis. *Invest Ophthalmol Vis Sci*. 2008;49:4078–4088.
21. Khankan R, Oliver N, He S, Ryan SJ, Hinton DR. Regulation of fibronectin-EDA through CTGF domain-specific interactions with TGFbeta2 and its receptor TGFbetaRII. *Invest Ophthalmol Vis Sci*. 2011;52:5068–5078.
22. Yokoyama K, Kimoto K, Itoh Y, et al. The PI3K/Akt pathway mediates the expression of type I collagen induced by TGF-beta2 in human retinal pigment epithelial cells. *Graefes Arch Clin Exp Ophthalmol*. 2012;250:15–23.
23. Itoh Y, Kimoto K, Imaizumi M, Nakatsuka K. Inhibition of RhoA/Rho-kinase pathway suppresses the expression of type I collagen induced by TGF-beta2 in human retinal pigment epithelial cells. *Exp Eye Res*. 2007;84:464–472.
24. Saika S, Yamanaka O, Ikeda K, et al. Inhibition of p38MAP kinase suppresses fibrotic reaction of retinal pigment epithelial cells. *Lab Invest*. 2005;85:838–850.
25. Ong CH, Bateman A. Progranulin (granulin-epithelin precursor, PC-cell derived growth factor, acrogranin) in proliferation and tumorigenesis. *Histol Histopathol*. 2003;18:1275–1288.
26. Hall MO, Obin MS, Heeb MJ, Burgess BL, Abrams TA. Both protein S and Gas6 stimulate outer segment phagocytosis by cultured rat retinal pigment epithelial cells. *Exp Eye Res*. 2005;81:581–591.
27. Hall MO, Prieto AL, Obin MS, et al. Outer segment phagocytosis by cultured retinal pigment epithelial cells requires Gas6. *Exp Eye Res*. 2001;73:509–520.
28. Hafizi S, Dahlback B. Gas6 and protein S. Vitamin K-dependent ligands for the Axl receptor tyrosine kinase subfamily. *FEBS J*. 2006;273:5231–5244.
29. Hafizi S, Dahlback B. Signalling and functional diversity within the Axl subfamily of receptor tyrosine kinases. *Cytokine Growth Factor Rev*. 2006;17:295–304.
30. Jeong EY, Kim S, Jung S, et al. Enhancement of IGF-2-induced neurite outgrowth by IGF-binding protein-2 and osteoglycin in SH-SY5Y human neuroblastoma cells. *Neurosci Lett*. 2013;548:249–254.
31. Li R, Maminishkis A, Wang FE, Miller SS. PDGF-C and -D induced proliferation/migration of human RPE is abolished by inflammatory cytokines. *Invest Ophthalmol Vis Sci*. 2007;48:5722–5732.
32. Nagineni CN, Kutty V, Detrick B, Hooks JJ. Expression of PDGF and their receptors in human retinal pigment epithelial cells and fibroblasts: regulation by TGF-beta. *J Cell Physiol*. 2005;203:35–43.
33. Leschey KH, Hackett SF, Singer JH, Campochiaro PA. Growth factor responsiveness of human retinal pigment epithelial cells. *Invest Ophthalmol Vis Sci*. 1990;31:839–846.
34. Weng CY, Kothary PC, Verkade AJ, Reed DM, Del Monte MA. MAP kinase pathway is involved in IGF-1-stimulated proliferation of human retinal pigment epithelial cells (hRPE). *Curr Eye Res*. 2009;34:867–876.
35. Spraul CW, Kaven C, Amann J, Lang GK, Lang GE. Effect of insulin-like growth factors 1 and 2, and glucose on the migration and proliferation of bovine retinal pigment epithelial cellsin vitro. *Ophthalmic Res*. 2000;32:244–248.
36. Grant MB, Guay C, Marsh R. Insulin-like growth factor I stimulates proliferation, migration, and plasminogen activator release by human retinal pigment epithelial cells. *Curr Eye Res*. 1990;9:323–335.
37. Ramasamy S, Narayanan G, Sankaran S, Yu YH, Ahmed S. Neural stem cell survival factors. *Arch Biochem Biophys*. 2013;534:71–87.
38. Julien S, Kreppel F, Beck S, et al. A reproducible and quantifiable model of choroidal neovascularization induced by VEGF A165 after subretinal adenoviral gene transfer in the rabbit. *Mol Vis*. 2008;14:1358–1372.
39. Zhao B, Ma A, Cai J, Boulton M. VEGF-A regulates the expression of VEGF-C in human retinal pigment epithelial cells. *Br J Ophthalmol*. 2006;90:1052–1059.
40. Ablonczy Z, Crosson CE. VEGF modulation of retinal pigment epithelium resistance. *Exp Eye Res*. 2007;85:762–771.

41. Hartnett ME, Lappas A, Darland D, McColm JR, Lovejoy S, D'Amore PA. Retinal pigment epithelium and endothelial cell interaction causes retinal pigment epithelial barrier dysfunction via a soluble VEGF-dependent mechanism. *Exp Eye Res*. 2003;77:593–599.
42. Byeon SH, Lee SC, Choi SH, et al. Vascular endothelial growth factor as an autocrine survival factor for retinal pigment epithelial cells under oxidative stress via the VEGF-R2/PI3K/Akt. *Invest Ophthalmol Vis Sci*. 2010;51:1190–1197.
43. Chu YK, Lee SC, Byeon SH. VEGF rescues cigarette smoking-induced human RPE cell death by increasing autophagic flux: implications of the role of autophagy in advanced age-related macular degeneration. *Invest Ophthalmol Vis Sci*. 2013;54:7329–7337.
44. Kaven CW, Spraul CW, Zavazava NK, Lang GK, Lang GE. Growth factor combinations modulate human retinal pigment epithelial cell proliferation. *Curr Eye Res*. 2000;20:480–487.
45. Gamulescu MA, Chen Y, He S, et al. Transforming growth factor beta2-induced myofibroblastic differentiation of human retinal pigment epithelial cells: regulation by extracellular matrix proteins and hepatocyte growth factor. *Exp Eye Res*. 2006;83:212–222.
46. Sugioka K, Kodama A, Okada K, et al. TGF-beta2 promotes RPE cell invasion into a collagen gel by mediating urokinase-type plasminogen activator (uPA) expression. *Exp Eye Res*. 2013; 115:13–21.
47. Ivanova VP, Kovaleva ZV, Anokhina VV, Krivchenko AI. The effect of the collagen tripeptide fragment (GER) on the adhesion and spreading of fibroblasts depends on the properties of adhesive surface [in Russian]. *Tsitologiia* 2012;54:823–830.
48. Sipes JM, Krutzsch HC, Lawler J, Roberts DD. Cooperation between thrombospondin-1 type 1 repeat peptides and alpha(v)beta(3) integrin ligands to promote melanoma cell spreading and focal adhesion kinase phosphorylation. *J Biol Chem*. 1999;274:22755–22762.
49. Ortega N, Werb Z. New functional roles for non-collagenous domains of basement membrane collagens. *J Cell Sci*. 2002;115:4201–4214.
50. Chen S, Birk DE. The regulatory roles of small leucine-rich proteoglycans in extracellular assembly. *FEBS J*. 2013;280:2120–2137.
51. Sarrazin S, Adam E, Lyon M, et al. Endocan or endothelial cell specific molecule-1 (ESM-1): a potential novel endothelial cell marker and a new target for cancer therapy. *Biochim Biophys Acta*. 2006;1765:25–37.
52. Iozzo RV, Schaefer L. Proteoglycans in health and disease: novel regulatory signaling mechanisms evoked by the small leucine-rich proteoglycans. *FEBS J*. 2010;277:3864–3875.
53. Farach-Carson MC, Brown AJ, Lynam M, Safran JB, Carson DD. A novel peptide sequence in perlecan domain IV supports cell adhesion, spreading and FAK activation. *Matrix Biol*. 2008;27:150–160.
54. Soulez M, Sirois I, Brassard N, et al. Epidermal growth factor and perlecan fragments produced by apoptotic endothelial cells co-ordinately activate ERK1/2-dependent antiapoptotic pathways in mesenchymal stem cells. *Stem Cells*. 2010;28: 810–820.
55. Lee B, Clarke D, Al Ahmad A, et al. Perlecan domain V is neuroprotective and proangiogenic following ischemic stroke in rodents. *J Clin Invest*. 2011;121:3005–3023.
56. van der Valk J, Brunner D, De Smet K, et al. Optimization of chemically defined cell culture media–replacing fetal bovine serum in mammalian in vitro methods. *Toxicology In Vitro*. 2010;24: 1053–1063.